Liquid Metal Strain Gage to Test Cervical Facet Capsule Strain

Haibin CHEN[1], Yi WANG[1,2], Liying ZHANG*[3], Guangyu YANG[1], Xin NING[1], Xuemei CHENG[1], Zhengguo WANG*[1]

[1]State Key Laboratory of Trauma, Burns, and Combined Injuries, Institute of Surgery Research, Daping Hospital, Third Military Medical University, Chongqing 400042, China, Ph./Fax: +86-23-68718064
[2]Electronic and Electrical Department, Beijing Automotive Technology Center, Beijing 100021, China, Ph./Fax: +86-23-68718064
[3]Bioengineering Center, Wayne State University, Detroit-Michigan 48202, USA, Ph./Fax: +1-313-205-3067
Corresponding author, e-mail: hoy.chen@yahoo.com, chenhb57474@163.com, lzhang@wayne.edu, 22517327@qq.com, ningxin48@tom.com, chengxm718@163.com, wangzhg@cae.cn*

Abstract

A broad range of investigations has been carried out to suggest that the facet joint capsule is a source of neck pain and the pain may arise from large strain in the cervical facet capsule that will cause pain receptors to fire. So far, no direct methods to in vivo test the cervical facet capsule strain during rear-end crashes have been known. To solve this methodology problem, a special liquid metal was selected as a sensing element to develop a miniature wire high-range strain gage. The calibration tests and a sled rear-end impact experiment were carried out to examine the technical behavior of this strain gage. It is shown that: This strain gage has a relatively high strain range and a relatively high degree of linearity. Due to a miniature wire structure and a relatively high degree of flexibility of use as well as a minimal external adhesive force, this strain gage has the capability of in vivo testing cervical facet capsule strain. In summary, this strain gage has a potential to become the first application research of liquid metal strain gage in testing cervical facet capsule strain during rear-end crashes.

Keywords: strain gage, neck pain, cervical spine, rear-end crash, liquid metal

1. Introduction

One of the most flexible regions of the spine is the neck region, which consists of vertebrae, seven load-absorbing discs, muscles, and vertebral ligaments to hold them in place [1]. The uppermost cervical disc connects the top of the spinal column to the base of the skull. The spinal cord, which sends nerve impulses to every part of the body, runs through a canal in the cervical vertebrae and continues all the way down the spine. The neck is considered to be one of natures most badly "designed" areas of the body. Upon impact, such as automotive or sports related collisions, the neck is vulnerable to injury. The vehicle injury priority rating data indicated that neck injuries became the fifth most important injury category (after head, face, chest and abdomen) [2]. Besides the high rate of neck related ailments in automotive accidents, long term neck pain and subsequent rehabilitation are often associated with rear-end collisions [3]-[4].

A broad range of investigations has been carried out to suggest that the facet joint capsule is a source of neck pain and the pain may arise from large strain in the joint capsule that will cause pain receptors to fire [5]-[8]. Morphologically, the cervical facet joint capsule is well innervated, receiving nerve supply from the medial branches of the dorsal rami, and each medial branch segmentally innervates at two facet joints [9]. Excessive facet capsule stretch, while not producing visible tearing, has been proved to produce functional plasticity of dorsal horn neuronal activity [10]. Studies using diagnostic blocks also suggest that many of cervical facet joint pain patients have no obvious radiographic abnormalities and pain may be of capsular origin [11]-[12].

It is apparent thus far that neck pain signals and capsule strain must be synchronously measured if neck pain mechanism in rear-end crashes is to be clearly understood. However, no

direct methods to in vivo test the cervical facet capsule strain during rear-end crashes have been known [13]-[16].

Due to a high range and a good flexibility, the miniature wire strain gage of the liquid metal type can be used for in vivo test of uneven surface strain. The purpose of this paper is to design a miniature wire strain gage of the liquid metal type and to provide a method for making this gage in a relatively simple but highly effective manner.

2. Research Method
2.1. Design principle

Since its resistivity (ρ) and volume (V) keep constant even under large strain conditions, a special liquid metal (SLM) was selected as a sensing element to design a miniature wire high-range strain gage (Figure 1).
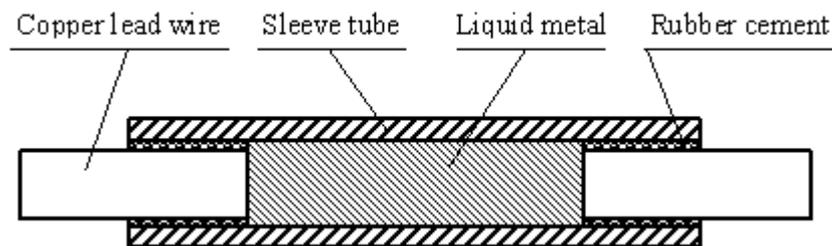
Figure 1. Scheme of the miniature strain gage of liquid metal

The gage consists of an elongated sleeve tube of elastic electrically non-conducting material, preferably rubber, of suitable length such, of example, as 12 mm with an inside diameter of 0.5 mm and filled with a SLM. Changes in the electrical resistance of the SLM column in response to elongation of the sleeve tube constitute a measure of strain.

An analysis of the gage is as follows: Using

$$R = \rho\,\frac{L}{A} \tag{1}$$

for this SLM column it can easily be shown that

$$R = \rho\,\frac{L}{A} = \frac{\rho}{V}\,L^2 \tag{2}$$

$$dR = 2\,\frac{\rho}{V}\,L\,dL \tag{3}$$

$$\frac{dR/R}{dL/L} = GF = 2 \tag{4}$$

where
R = Resistance of SLM column
ρ = Resistivity of SLM column
L = Length of SLM column = Effective length of this strain gage
A = Uniform cross sectional area of SLM column
GF = Gage factor (unit change in resistance per unit change in length).

Assume that △R and △L represent the electric resistance change and length change of SLM column under test, respectively. The average strain (ε) of the SLM column can be expressed as

$$\varepsilon = \frac{\Delta L}{L} = \frac{1}{2}\frac{\Delta R}{R} = \frac{\Delta R}{R}/GF \tag{5}$$

In this study, a D.C. single-arm Wheatstone Bridge was used for the measuring operation of ε.

2.2. Strain measurement circuit

The complete strain measuring chain is shown in the schematic drawing in Figure 2.
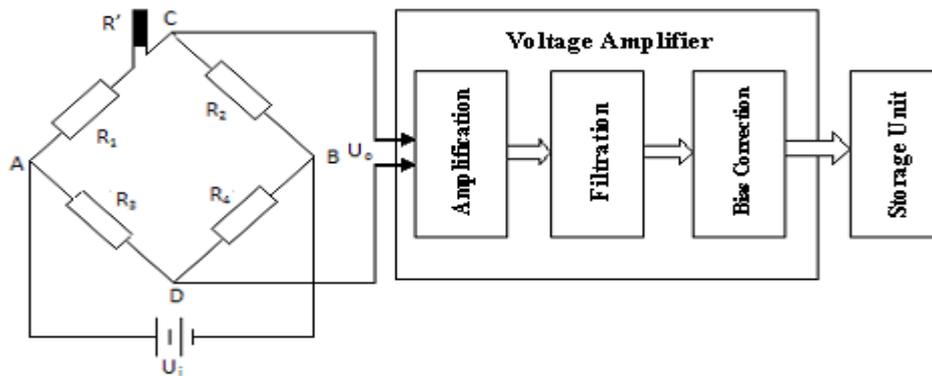
Figure 2. Schematic drawing of a strain measuring chain with an SLM strain gage

Figure 3. Calibration setup of Sample 1(see online version for colours)

The strain gage is incorporated into a D.C. single-arm Wheatstone Bridge, and a specially-made voltage amplifier is used to measure quite small changes of the gage resistance

(e.g. $\Delta R' \approx 0.16\,\Omega$ and $U_o \approx$ 2mV when $\varepsilon = 100\%$)[17]-[18]. Here, R' and R_g ($R_g = R_1 = R_2 = R_3 = R_4$ = 100 Ohms) signify the resistance of this strain gage and the bridge arms, respectively; and U_i and U_o signify the power supply voltage and output voltage of the bridge circuit (U_i = 5V), respectively.

2.3. Strain gage calibration
Calibration setup. An Instron 8871 testing machine (Figure 3) was applied to calibrate three custom-made strain gage samples (Samples I and II and III). Among them, Sample I was used to carry out the gage application experiment (Figure 3). The ambient environmental conditions under the static calibration had been established as follows: (a) temperature: 22.5 ; (b) relative humidity: 55%; and (c) barometric pressure: 980 kPa.

Calibration procedure. The strain gages are calibrated by a procedure with stepwise loading and unloading strains. A schematic drawing of the load variation as a function of the measuring time *t* is shown in Figure 4.
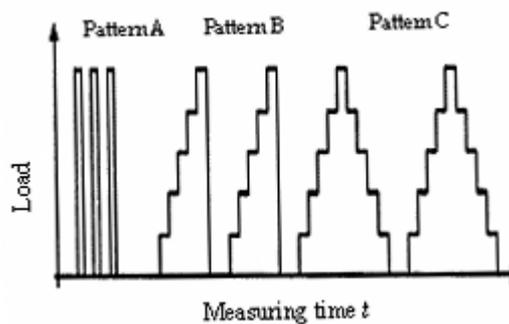
Figure 4. Calibration loading pattern
(Pattern A: three preloads; Pattern B: for Sample I; Pattern C: for Sample II and III)

After three preloads (i.e. Pattern A), perform two complete calibration cycles consecutively---just like Pattern B or Pattern C. Each cycle consists of strain increments up to the upper limit of the calibrated range followed by strain decrements down to the lower limit of the calibrated range.

Calibration equations. Perform a least-squares linear regression analysis on the calibration point data where values of applied strain from the INSTRON 8871 are (*x*) and system output is (*y*). That is, $x = \varepsilon$, $y = U_{os}/U_i$. Here U_{os} is the output voltage of the whole measuring system. Compute the correlation coefficient (R^2 or *r*); and compute the intercept (b) and the slope (a) to get the calibration equation:

$$y = a\,x + b \tag{6}$$

or

$$y = a\,x \tag{7}$$

2.4. Strain gage application
To determine the test capability of this miniature strain gage, a 14.34-kph sled rear-end impact test was carried out (Figures 5 and 7(a)). In this test setup, a physical head-neck model (PM) similar to living goats was used as a human surrogate (Figure 5). The backward facing instrumented PM was fixed on a rigid seatback at a 20° seatback angle, and a posture control device was used to assure that its head-neck moved along a prescribed trace within the saggital plane during impacts. The deceleration sled had a carriage that was mounted on a sled track [19]. This carriage was a 600 kilogram standard platform and was propelled by means of a programmable linear drive, the closed-loop linear direct current motor drive system.

The required sled deceleration pulse was then achieved by means of re-usable polyurethane tube devices placed in parallel inside steel pipes, which were rigidly attached to the fixed crash barrier wall. Deceleration occurred when five steel shafts on the sled carriage, which were fitted with olive-shaped ends, were rammed inside the polyurethane tubes, absorbing the impact energy.

Figure 5. Instrumented PM (see online version for colours)
(A_H: acceleration gage of PM head; S_N: strain gage of PM neck)

Lateral high-speed digital video (at 1000 fps) was taken of each sled test to observe the PM responses (Figure 7(a)). Measurements of head acceleration and neck strain of this physical model were also carried out during the tests when the appropriate instrumentation was fitted (Figures 5 and 7(a)).

3. Results and Analysis
3.1. Strain gage calibration results
Figure 6 shows that this strain gage has a relatively high strain range (i.e. up to 187.7% for Sample III) and a relatively high degree of linearity (i.e. R^2 = 0.9559, 0.9764, 0.9963 for Samples I and II and III, respectively.).

3.2. Strain gage application results
Figure 7 illustrates the impact responses of the physical head-neck model in the rear-end crashes, while Figure 8 reveals the high-speed photo images subject to t = t_0 and t_1 and t_2.

From Figure 7 and Figure 8, it is shown that: during t_0 to t_2, the neck dis-responses have similar variation trend to head Ax & Az responses and neck high-speed photo images, representing that this miniature strain gage was able to successfully "capture" the strain signals of cervical facet capsule.

3.3. Performance analysis of this liquid metal strain gage
(a) Image analysis method vs **this liquid metal strain gage test method.** To date, the former is the main method to test cervical facet capsule strain. The operation principle of the former is as follows: First, infrared micro-balls were attached to the cervical facet capsules as

photo markers, and a complicated stereoimaging system was incorporated to track capsular deformation during mechanical tests or crash simulations.
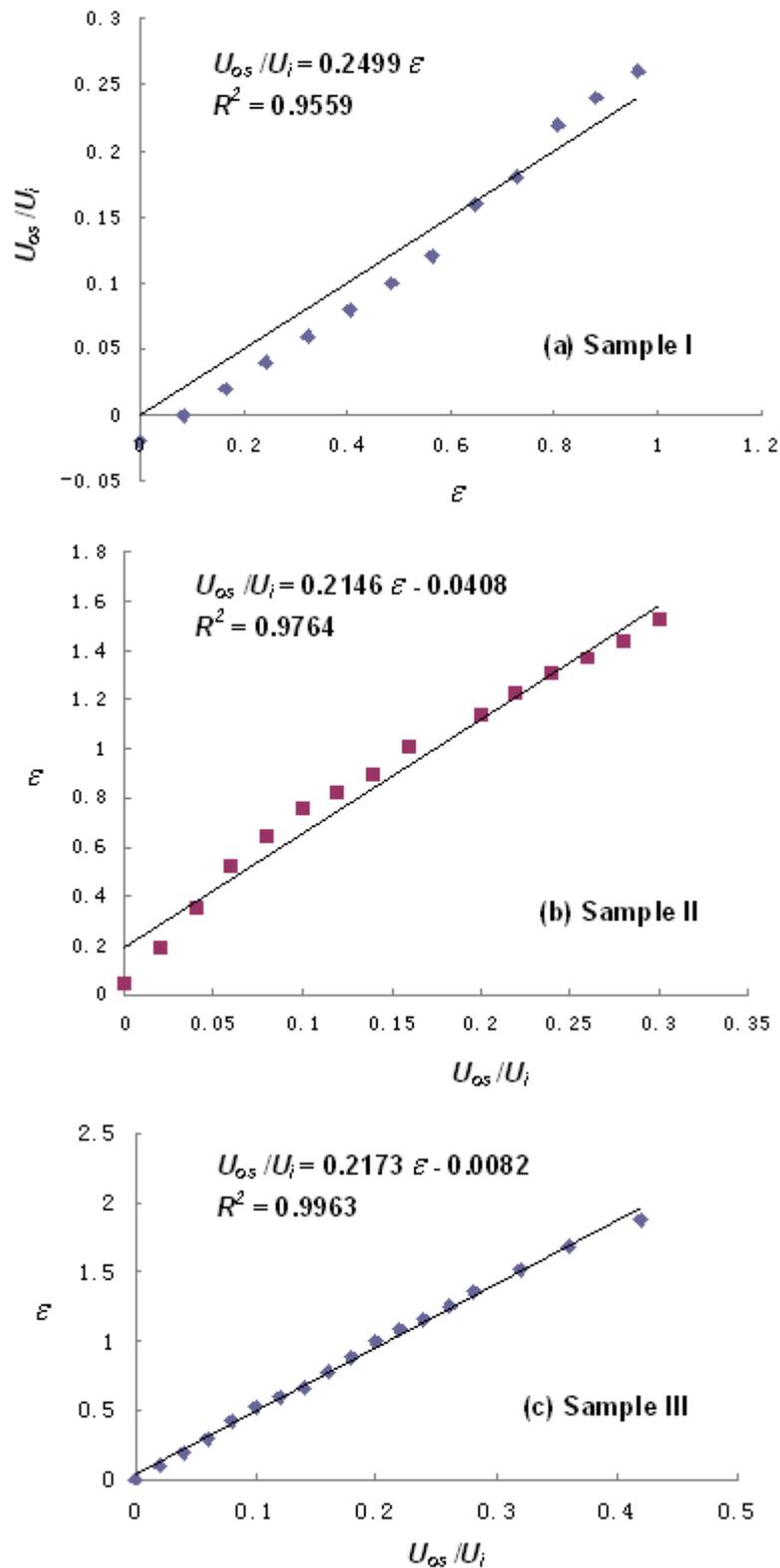
Figure 6. Calibration equation of Calibration curve of three strain gage samples
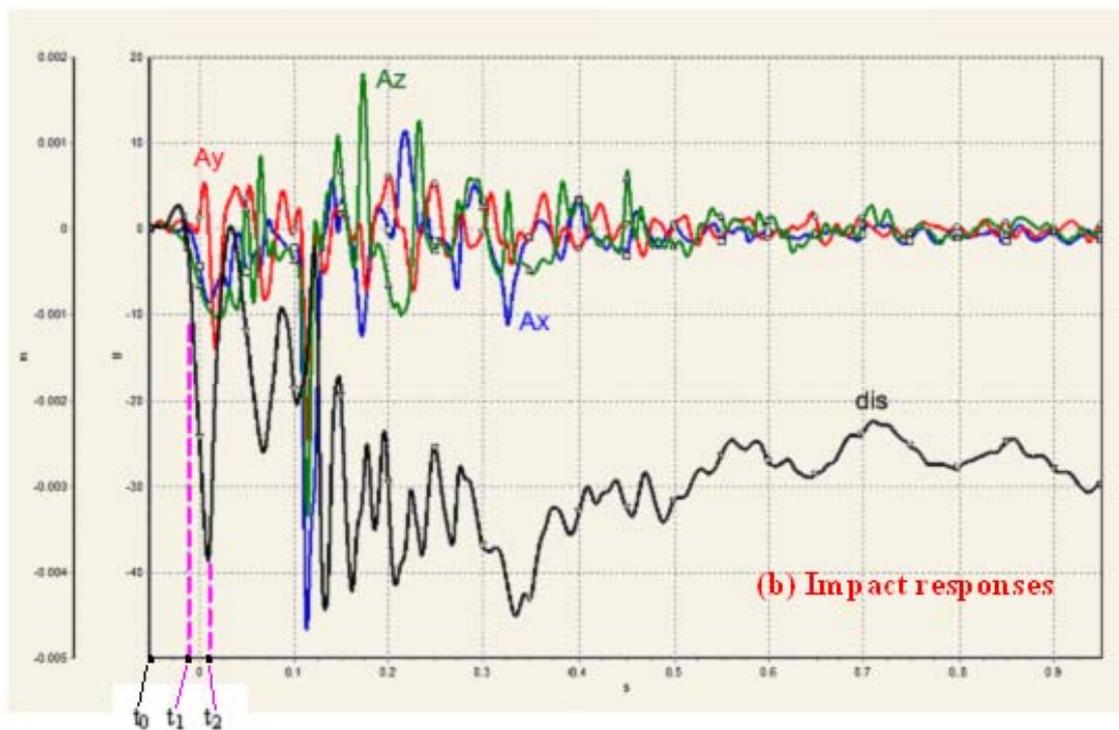
Figure 7. Impact responses of the PM during the rear-end crash
(**Ax** and **Az**: head acceleration components which are mutually orthogonal in the saggital plane; **Ay**: head acceleration component vertical to the saggital plane. **dis**: neck tensile displacement; see online version for colours)
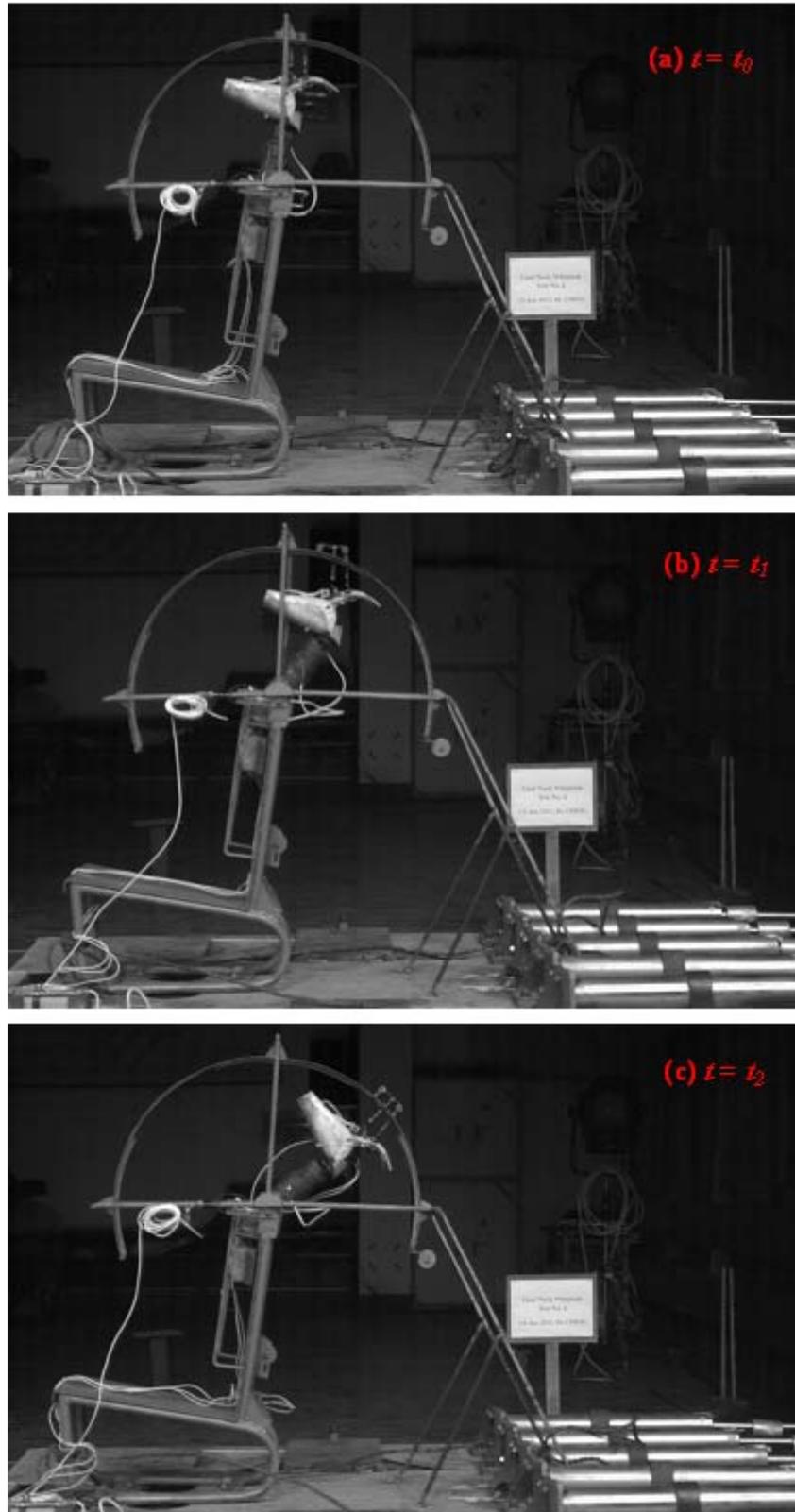
Figure 8. High-speed photo images of the PM during the rear-end crash
(see online version for colours)

3.3. Performance analysis of this liquid metal strain gage (*Contd*)

(a) Image analysis method vs this liquid metal strain gage test method (*Contd*). Second, marker positions in the stereo images were manually digitized using customized software with a centroid-finding algorithm. The three dimensional coordinates of all markers were reconstructed from the digitized marker positions in the stereo images using direct linear transformation (DLT). Third, an array (i.e. 4×4, 4×5 or 5×5) of markers was treated as nodes of a four node isoparametric element. By tracking the grid of capsular markers and applying FEM analysis, the strain distribution was obtained for the related elements in each test. Obviously, it is difficult to in vivo test the cervical facet capsule strain during rear-end crashes by means of this image analysis method.

Correspondingly, the later has three advantages the following: First, this strain gage is relatively simple and economical in construction (Figures 1-3). Second, this strain gage is relatively convenient in operation. Shown as Eq.5, the measure, namely "average strain (ε) of the whole target zone", was directly measured to represent the strain characteristics of the target zone. Third, due to a miniature wire structure and a high degree of flexibility of use as well as a minimal external adhesive force, this strain gage has the capability of in vivo testing cervical facet capsule strain. Little reports similar to the strain gage methodology stated in this paper have been known.

(b) Previous liquid metal strain gages vs this liquid metal strain gage. The former has been primarily applied to test the vibration responses of metal structures in the mechanical engineering field. Correspondingly, the later has a potential to become the first application research of liquid metal strain gage in testing cervical facet capsule strain during rear-end crashes.

3.4. Limitation of this study

(a) Leakage of the SLM. Shown as Figure 1, two copper lead wires were secured in the SLM filled tube. Electrical connections are made to the ECL column by means of lead wires, which also seal the ends of the sleeve tube by mean of rubber cement. Unfortunately, the sleeve tube of Sample 1 has a disadvantage of SLM leakage four months after test.

(b) Lack of gage bonding methodology. Due to the varied size and uneven surface of the capsules, it was difficult to maintain a uniform three dimensional deformation. Under the actual rear-end crash test applications the sleeve tube might be secured at its ends to a cervical facet capsule to extension or the tube may be, as is usually the case, bonded throughout its effective length to this capsule surface. However, this study had not provided a clear bonded manner--- whether the two ends or throughout the effective length of this gage or others?

4. Conclusion

The main contributions of this study comprised of three aspects, the first of which is that a bonded miniature wire high-range strain gage of the liquid metal type was developed. The second aspect is that a method for making this gage in a relatively simple but highly effective manner was established. The third aspect is that this strain gage has a potential to become the first application research of liquid metal strain gage in testing cervical facet capsule strain during rear-end crashes.

The object of further researches is to provide an improved type of the liquid metal strain gage stated in this paper that has extraordinary elongation combined with a high degree of accuracy, sensitivity and ease of application.

References

[1] Chen HB, Zhang LY, Tan LW, Zhang SX, Cheng XM, Wang ZG. Comparative Analysis of Chinese and Western Cervical Vertebrae Geometry. *TELKOMNIKA Indonesian Journal of Electrical Engineering*. 2012; 10: to be published in December 2012.

[2] King AI. Fundamentals of impact biomechanics: part 1–biomechanics of the head, neck, and thorax. *Annu. Rev. Biomed. Eng*. 2000; 2: 55-81.

[3] Chen HB, Zhang LY, Wang ZG, Cavanaugh JM, Yang KH. *Editors*. Biomechanics and Neurophysiology of Cervical Facet Joint Pain. New York: Nova Science Publishers, Inc. 2011.

[4] Chen HB, Yang K, Wang ZG. Biomechanics of whiplash injury. *Chin J Traumatol.* 2009; 12(5): 305-314.

[5] Yang K, Begeman P. *A proposed role for facet joints in neck pain in low to moderate speed rear end impacts Part I: Biomechanics*. 6th Injury Prevention Through Biomechanics Symposium. What-city, what-country. 1996; 59-63.

[6] Deng B, Begeman P, Yang K, Tashman S, King A. Kinematics of human cadaver cervical spine during low speed rear-end impacts. *Journal of Stapp Car Crash*. 2000; 44: 171-188.

[7] Luan F, Yang K, Deng B. Qualitative analysis of neck kinematics during low-speed rear-end impact. *Clin Biomech*. 2000; 15(9): 649-657.

[8] Panijabi M, Cholewicki J, Nibu K, Grauer J, Vahldiek M. Capsular ligament stretches during in vitro whiplash simulations. *J Spinal Disord*. 1998; 11: 227-232.

[9] Bogduk N. The clinical anatomy of the cervical doral rami. *Spine*. 1982; 7: 319-330

[10] Quinn KP, Dong L, Golder FJ, Winkelstein BA. Neuronal hyperexcitability in the dorsal horn after painful facet joint injury. *Pain*. 2010; 151(2): 414-421.

[11] Bogduk N, Marsland A. The cervical zygapophysial joints as a source of neck pain. *Spine*. 1988; 13(6): 610-617.

[12] Aprill C, Bogduk N. The prevalence of cervical zygapophyseal joint pain: a first approximation. *Spine*. 1992; 17: 744-747.

[13] LU Y. *Neural response of cervical facet joint capsule to stretch: a potential whiplash pain mechanism*. Wayne State University. Detroit, USA. 2006.

[14] Cavanaugh J, Ozaktay A, Yamashita T, Avramov A, Getchell T, King A. Mechanisms of low back pain: a neurophysiologic and neuroanatomic study. *Clin Orthop Relat Res*. 1997; 335: 166-180.

[15] Chen C, Lu Y, Cavanaugh J, Kallakuri S, Patwardhan A. Recording of neural activity from goat cervical facet joint capsule using custom-designed miniature electrodes. *Spine*. 2005; 30(12): 1367-1372.

[16] Lee K, Davis M, Mejilla R, Winkelstein B. In vivo cervical facet capsule distraction: mechanical implications for whiplash and neck pain. *Journal Stapp Car Crash*. 2004; 48: 373-395.

[17] Hartati S, Harjoko A, Supardi TW. The Digital Microscope and Its Image Processing Utility. *TELKOMNIKA Indonesian Journal of Electrical Engineering*. 2011; 9(3): 565-574.

[18] Samosir AS. Development of a Current Control Ultracapacitor Charger Based on Digital Signal Processing. *TELKOMNIKA Indonesian Journal of Electrical Engineering*. 2009; 7(3): 145-150.

[19] Chen HB, Wang ZG, Yin ZY, Li SH, Li XY, Nin X. Development of a precision welded impact sled test track. *Int. J. Vehicle Systems Modelling and Testing*. 2012; 7(1): 73-103.